A Remarkable Isostructural Homologous Series of Mixed Lithium−Heavier Alkali Metal *tert*-Butoxides [(*t*-BuO)$_8$Li$_4$M$_4$] (M = Na, K, Rb or Cs)

David R. Armstrong,[†] William Clegg,[‡] Allison M. Drummond,[†] Stephen T. Liddle,[‡] and Robert E. Mulvey*,[†]

Contribution from the Department of Pure and Applied Chemistry, University of Strathclyde, Glasgow G1 1XL, U.K, and the Department of Chemistry, University of Newcastle, Newcastle upon Tyne NE1 7RU, U.K.

Received June 21, 2000

Abstract: Three new mixed lithium−heavier alkali metal *tert*-butoxides [(*t*-BuO)$_8$Li$_4$M$_4$] (M = Na, Rb, Cs) are reported which, added to the previously discovered potassium analogue [(*t*-BuO)$_8$Li$_4$*K*$_4$], complete the homologous series. Remarkably, X-ray crystallographic studies reveal that all four heterometallic compounds adopt a common structure. This sixteen-vertex O$_8$Li$_4$M$_4$ "breastplate" motif is built around novel (M$^+$)$_4$ planes (M = Na, K, Rb, Cs), both faces of which support chelating (O$_4$Li$_2$)$^{2-}$ dianions. Each such dianion is positioned approximately normal with respect to the other. Bonding within the breastplate structure involves a combination of μ_3-Li, μ_4-M, μ_3-O, and μ_4-O centers. Ab initio MO calculations on model systems predict that formation of the heterometallic breastplate from the exclusively μ_3-bonded frameworks of its component homometallic structures is a favorable exothermic process. Best regarded as an inherently stable contacted triple ion sandwich comprising a dianion−tetramonocation−dianion arrangement, the breastplate motif is likely to be more widely applicable within heterometallic structural chemistry than so far recognized. This point is discussed with reference to a previously documented series of heterometallic p-block metal-based imide structures of general formula [(CyN)$_8$M$^1_4$M$^2_4$], where M^1 = Sb or As and M^2 = Ag, Cu, or Na.

Introduction

While recent times have witnessed a gigantean rise in the number of crystallographically characterized organoelement−alkali metal structures,[1] it is still rare to find among them complete sets of homologous series (i.e., RM, where M = Li, Na, K, Rb, or Cs).[2] Furthermore, such a homologous series would not be expected to be isostructural in view of the significant size gradation that runs through Group 1.[3] Clear-cut differences in aggregation state, and/or in the nature and extent of solvation, and/or in coordination number are the norm. Illustrative of this point and germane to the new compounds reported herein, whereas the heavier alkali metal *tert*-butoxides *t*-BuOK,[5] *t*-BuORb,[5] and *t*-BuOCs[6] form isotypic, tetrameric structures, the lithium congener *t*-BuOLi[7] is hexameric and the sodium congener *t*-BuONa[8] is both hexameric and nonameric in the same crystal. Hence, while the report of any newly discovered homologous series would be a welcome addition to the chemical literature, the one described here is all the more remarkable for the unique isostructural relationship that exists between its members. The first member, the tetralithium−tetrapotassium alkoxide [(*t*-BuO)$_8$Li$_4$K$_4$] (**1**), was the subject of a recent preliminary communication.[9] Here, in this paper, we reveal the successful synthesis and crystallographic characterization of the tetrasodium [(*t*-BuO)$_8$Li$_4$Na$_4$] (**2**), tetrarubidium [(*t*-BuO)$_8$Li$_4$Rb$_4$] (**3**), and tetracesium [(*t*-BuO)$_8$Li$_4$Cs$_4$] (**4**) analogues to complete the isostructural lithium−heavier alkali metal homologous series. To the best of our knowledge, no precedent exists within organoelement chemistry for such a mixed alkali metal−alkali metal homologous series. The complete set of heterometallic alkali metal−tin(II) *tert*-butoxide [M(*t*-BuO)$_3$Sn] structures has been documented previously,[10] but these show the expected structural demarcation: where M = Li or Na, a molecular arrangement is found; where M = K, Rb, or Cs, a polymeric arrangement is preferred. Our surprise finding here of a novel isostructural class of heterometallic demonstrates the importance of developing further the fundamental chemistry of alkoxides. There are also incentives for

[†] University of Strathclyde.

[‡] University of Newcastle.

(1) See the Cambridge Structural Database: Allen, F. H.; Kennard, O. *Chem. Des. Autom. News* **1993**, *8*, 1, 31.

(2) For some examples of such homologous series see: (a) Kottke, T.; Stalke, D. *Organometallics* **1996**, *15*, 4552. (b) Hoffmann, D.; Bauer, W.; Schleyer, P. v. R.; Pieper, U.; Stalke, D. *Organometallics* **1993**, *12*, 1193. (c) Pauer, F.; Stalke, D. *J. Organomet. Chem.* **1991**, *418*, 127. (d) Steiner, A.; Stalke, D. *Inorg. Chem.* **1993**, *32*, 1977. (e) Edelmann, F. T.; Pauer, F.; Wedler, M.; Stalke, D. *Inorg. Chem.* **1992**, *31*, 4143. (f) Klinkhammer, K. W. *Chem. Eur. J.* **1997**, *3*, 1418.

(3) Mingos, D. M. P. *Essential Trends in Inorganic Chemistry*; Oxford University Press: New York, 1998.

(4) For a review of lithium structures see: Setzer, W. N.; Schleyer, P. v. R. *Adv. Organomet. Chem.* **1985**, *24*, 353. For a review of heavier alkali metal structures see: Schade, C.; Schleyer, P. v. R. *Adv. Organomet. Chem.*, **1987**, *27*, 169.

(5) (a) Weiss, E.; Alsdorf, H.; Kühr, H. *Angew. Chem.* **1967**, *79*, 816; *Angew. Chem., Int. Ed.* **1967**, *6*, 801. (b) Weiss, E.; Alsdorf, H.; Kühr, H.; Grützmacher, H.-F. *Chem. Ber.* **1968**, *101*, 3777. (c) Chisholm, M. H.; Drake, S. R.; Naiini, A. A.; Streib, W. E. *Polyhedron* **1991**, *10*, 337.

(6) Mann, S.; Jansen, M. *Z. Kristallogr.* **1994**, *209*, 852.

(7) Thomas, R. D.; Bott, S. G.; Gravelle, P. W.; Nguyen, H. D. *Abstracts of the American Chemical Society, 215th ACS National Meeting, Dallas, 1998*; American Chemical Society: Washington, DC, 1998; INOR 291.

(8) Davies, J. E.; Kopf, J.; Weiss, E. *Acta Crystallogr.* **1982**, *B38*, 2251.

(9) Clegg, W.; Drummond, A. M.; Liddle, S. T.; Mulvey, R. E.; Robertson, A. *Chem. Commun.* **1999**, 1569.

(10) Veith, M.; Rösler, R. *Z. Naturforsch* **1986**, *41b*, 1071.

10.1021/ja002217z CCC: $19.00
Published on Web 10/27/2000

studying alkoxides within applied research as, for example, they find utility as precursors to technologically important oxide materials through chemical vapor deposition (CVD) or sol-gel processes,[11] and as active co-components of the "RLi·R′OK" type superbases commonly utilized in organic synthesis.[12]

Results and Discussion

Synthesis. In a strategy used in the past to prepare alkali metal−non-alkali metal heterometallic alkoxides,[13] lithium *tert*-butoxide and the appropriate heavier alkali metal congener are simply mixed together to afford the new all alkali metal *tert*-butoxides **1**−**4** (eq 1). Stoichiometric (1:1, *t*-BuOLi: *t*-BuOM molar ratios) conditions need not necessarily be employed, as the same products, usually in an improved crystalline form, can be obtained from lithium rich 2:1 molar ratios.

$$t\text{-BuOLi} + t\text{-BuOM} \rightarrow {}^{1}/_{4}[(t\text{-BuO})_8\text{Li}_4\text{M}_4] \qquad (1)$$

$$(\text{where M} = \text{Na, K, Rb, or Cs})$$

Yields were not optimized as the primary objective was to cultivate crystals of a quality suitable for X-ray crystallographic characterization. The reactions were carried out in toluene solution to which were added stoichiometric quantities (1 or 2 molar equiv per mol of *t*-BuOLi) of the coordinating solvent TMEDA (*N*,*N*,*N*′,*N*′-tetramethylethylenediamine, $Me_2NCH_2CH_2NMe_2$). Next the solutions were pumped to dryness in vacuo, and the residues were recrystallized from neat hexane solution. The heterometallic products crystallize *au naturel* in the sense that they do not contain TMEDA solvent ligands. In the preliminary report of **1** we speculated upon the idea that TMEDA molecules might catalyze the formation of the 16-vertex "breastplate" architecture (vide infra) though they themselves do not ultimately bind to it. This speculation can now be dismissed as **1** has been successfully reprepared in the absence of the diamine cosolvent. However, the employment of TMEDA was continued in the later preparations of **2**−**4** as its presence appears to aid the crystallization process somehow. It must be stressed that scrupulously anhydrous and anaerobic conditions are mandatory for the successful synthesis of **1**−**4**. Curiously, the lithium−rubidium alkoxide system is by far the most sensitive in this regard: despite seemingly applying all the usual precautions to prevent moisture and oxygen contamination, the synthesis of **3** could not always be reproduced. The presence of such contaminants encourages the formation of alternative heterometallic formulations containing oxygen-based anions as typified by the octalithium−dirubidium mixed alkoxide−hydroxide $[\{(t\text{-BuOLi})_7(\text{BuORb})_2(\text{LiOH})\cdot\text{TMEDA}\cdot\text{hexane}\}_\infty]$[14] and the heptalithium−tetrarubidium mixed alkoxide−peroxide $[\{(t\text{-BuOLi})_5(t\text{-BuORb})_4(\text{Li}_2\text{O}_2)\cdot(\text{TMEDA})_2\}_\infty]$.[15] Located at the core of the structure, these oxygen-based anions seem to act as templating seeds, from and around which grow three-dimensional cage structures of markedly different architectures to the breastplate design described here for **1**−**4** (vide infra). This concept of salt-molecule templation is an emerging feature within different areas of lithium−ligand coordination chemistry and includes ligands such as amidinates,[16] cresylates,[17] diazasulfates,[18] and phosphanides,[19] to name but a few. It has also surfaced in other mixed alkali metal−alkali metal *tert*-butoxide systems such as the tetralithium−pentapotassium mixed alkoxide−enolate−hydroxide $[(C_6H_{11}O)_4(t\text{-BuO})_4\text{Li}_4\text{K}_4\cdot\text{KOH}\cdot(\text{THF})_5]$[20] and the octalithium−dipotassium mixed alkoxide−oxide $[(t\text{-BuO})_8(\text{O})\text{Li}_8\text{K}_2\cdot(\text{TMEDA})_2]$.[21]

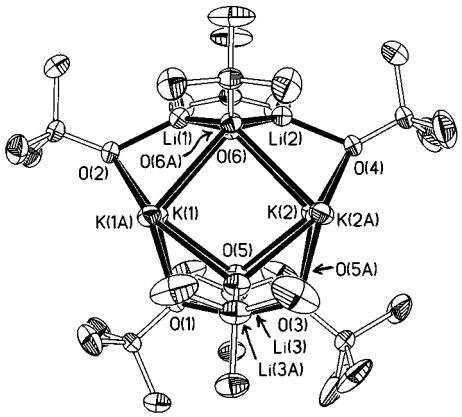

Figure 1. Molecular structure of **1** showing atom labeling for the $O_8Li_4K_4$ breastplate core. Hydrogen atoms have been omitted for clarity, and ellipsoids are at 40% probability.

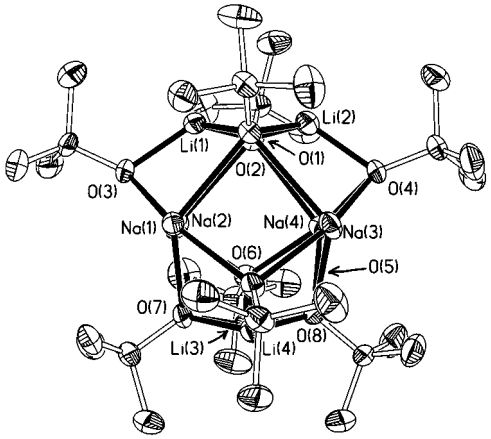

Figure 2. Molecular structure of one of the unique molecules of **2** showing atom labeling for the $O_8Li_4Na_4$ breastplate core. Hydrogen atoms have been omitted for clarity, and ellipsoids are at 40% probability.

The "Breastplate" Architecture. X-ray crystallographic studies have confirmed that the molecular structures of the new homologous series **1**−**4** are isostructural. This can be clearly seen by comparing the four individual structures shown in Figures 1−4, respectively, the views of which highlight their common 16-vertex, breastplate-like architecture. An alternative view of the generic structure is given in Figure 5. Exhibiting exact (or approximate in the case of structure **2**) crystallographic C_s symmetry and essentially D_{2d} symmetry for the molecule overall, this structure has two perpendicular mirror planes each running through two Li and four O atoms, and two C_2 axes

(11) (a) Bradley, D. C. *Chem. Rev.* **1989**, *89*, 1317. (b) Herrmann, W. A.; Huber, N. W.; Runte, O. *Angew. Chem.* **1995**, *106*, 2371; *Angew. Chem., Int. Ed. Engl.* **1995**, *34*, 2187.

(12) Lochmann, L. *Eur. J. Chem.* **2000**, 1115.

(13) (a) Mehrotra, R. C.; Singh, A.; Sogani, S. *Chem. Soc. Rev.* **1994**, *23*, 215. (b) Veith, M.; Mathur, S.; Mathur, C. *Polyhedron* **1998**, *17*, 1005.

(14) Clegg, W.; Drummond, A. M.; Liddle, S. T.; Mulvey, R. E. Unpublished results.

(15) Clegg, W.; Drummond, A. M.; Mulvey, R. E.; Liddle, S. T. *Chem. Commun.* **1998**, 2391.

(16) Kennedy, A. R.; Mulvey, R. E.; Rowlings, R. B. *J. Am. Chem. Soc.* **1998**, *120*, 7816.

(17) Henderson, K. W.; Mulvey, R. E.; Reinhard, F. B. M.; Clegg, W.; Horsburgh, L. *J. Am. Chem. Soc.* **1994**, *116*, 10777.

(18) Brask, J. K.; Chivers, T.; Yap, G. P. A. *Inorg. Chem.* **1999**, *38*, 5588.

(19) Driess, M. *Acc. Chem. Res.* **1999**, *32*, 1017.

(20) Williard, P. G.; MacEwan, G. J. *J. Am. Chem. Soc.* **1989**, *111*, 7671.

(21) Mackenzie, F. M.; Mulvey, R. E.; Clegg, W.; Horsburgh, L. *Polyhedron* **1998**, *17*, 993.

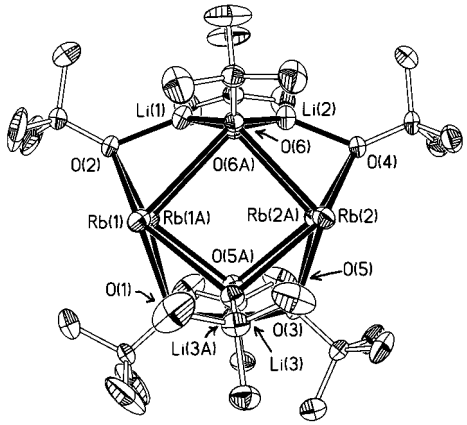

Figure 3. Molecular structure of **3** showing atom labeling for the $O_8Li_4Rb_4$ breastplate core. Hydrogen atoms have been omitted for clarity, and ellipsoids are at 40% probability.

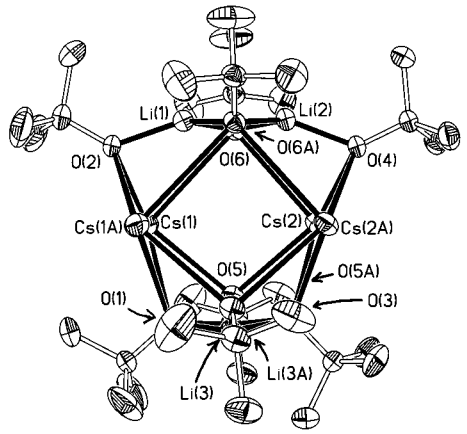

Figure 4. Molecular structure of **4** showing atom labeling for the $O_8Li_4Cs_4$ breastplate core. Hydrogen atoms have been omitted for clarity, and ellipsoids are at 40% probability.

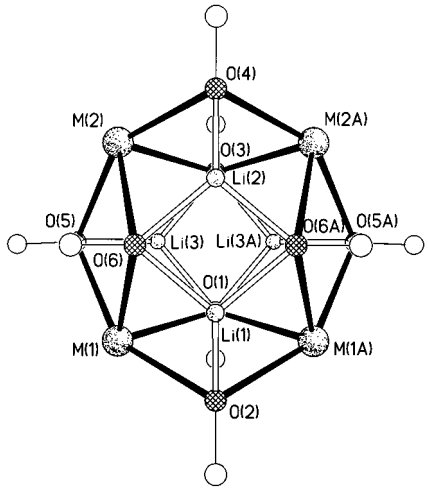

Figure 5. Alternative view of the generic breastplate structure.

running through pairs of opposite M atoms. Figure 5 is viewed along the S_4 axis. The metal−oxygen framework comprises 14 four-membered rings, arranged in three distinct sets: 8(OLiOM), $4(OM)_2$, and $2(OLi)_2$. All of these rings are nonplanar. The two $(OLi)_2$ "neck" and "waist" rings are disposed approximately orthogonal to each other. Separating these rings in the "midriff" region is a perfect plane of four heavier alkali metal cations (M^+). The eight oxygen centers within the breastplate surround the smaller Li^+ cations in trigonal pyramidal LiO_3 coordination

Table 1. Selected Bond Lengths (Å) and Angles (deg) for Compound **1**[a]

Bond Lengths			
K(1)−O(2)	2.6435(11)	K(1)−O(5)	2.6447(12)
K(1)−O(6)	2.8425(11)	K(1)−O(1)	2.8492(11)
K(2)−O(4)	2.6366(11)	K(2)−O(5)	2.6472(12)
K(2)−O(3)	2.8768(11)	K(2)−O(6)	2.9309(11)
Li(1)−O(2)	1.828(4)	Li(1)−O(6)	1.918(3)
Li(2)−O(4)	1.824(4)	Li(2)−O(6)	1.910(3)
Li(3)−O(5)	1.815(3)	Li(3)−O(3)	1.911(3)
Li(3)−O(1)	1.919(3)		

Bond Angles			
O(2)−K(1)−O(5)	150.73(4)	O(2)−K(1)−O(6)	73.11(4)
O(5)−K(1)−O(6)	90.07(3)	O(2)−K(1)−O(1)	89.80(3)
O(5)−K(1)−O(1)	72.56(3)	O(6)−K(1)−O(1)	108.21(4)
O(4)−K(2)−O(5)	148.75(4)	O(4)−K(2)−O(3)	90.85(3)
O(5)−K(2)−O(3)	72.55(3)	O(4)−K(2)−O(6)	71.72(4)
O(5)−K(2)−O(6)	88.14(3)	O(3)−K(2)−O(6)	108.07(4)
O(2)−Li(1)−O(6)	121.71(13)	O(6A)−Li(1)−O(6)	99.42(18)
O(4)−Li(2)−O(6)	122.23(12)	O(6)−Li(2)−O(6A)	99.93(18)
O(5)−Li(3)−O(3)	122.95(15)	O(5)−Li(3)−O(1)	121.30(15)
O(3)−Li(3)−O(1)	99.29(13)	Li(3A)−O(1)−Li(3)	79.06(17)
Li(3A)−O(1)−K(1)	130.28(10)	Li(3)−O(1)−K(1)	78.02(8)
K(1)−O(1)−K(1A)	84.28(4)	Li(1)−O(2)−K(1)	84.62(9)
K(1A)−O(2)−K(1)	92.63(5)	Li(3)−O(3)−Li(3A)	79.47(17)
Li(3)−O(3)−K(2)	76.83(8)	Li(3)−O(3)−K(2A)	128.35(10)
K(2)−O(3)−K(2A)	83.13(4)	Li(2)−O(4)−K(2)	86.24(9)
K(2A)−O(4)−K(2)	92.75(5)	Li(3)−O(5)−K(1)	85.47(9)
Li(3)−O(5)−K(2)	84.75(9)	K(1)−O(5)−K(2)	94.06(4)
Li(2)−O(6)−Li(1)	78.76(13)	Li(2)−O(6)−K(1)	128.58(11)
Li(1)−O(6)−K(1)	77.64(11)	Li(2)−O(6)−K(2)	76.62(11)
Li(1)−O(6)−K(2)	129.23(11)	K(1)−O(6)−K(2)	84.23(3)

[a] Symmetry transformations used to generate equivalent atoms. A: $x, -y + {}^1/_2, z$.

polyhedra, and the larger M^+ cations in MO_4 coordination polyhedra intermediate between an apically vacant square-based pyramid and an equatorially vacant trigonal bipyramid. As a result there exists two distinct sets of oxygen centers: O(2), O(4), O(5), O(5A) are tricoordinate binding to one Li^+ and two M^+ cations; O(1), O(3), O(6), O(6A) are tetracoordinate binding to two Li^+ and two M^+ cations. Alkyl offshoots emanating from the polar $O_8Li_4M_4$ core complete the structure.

Selected bond lengths and bond angles for **1**−**4** are given in Tables 1−4, respectively. Associated crystallographic data are listed collectively in Table 5. Two essentially identical molecules were found in the asymmetric unit of the sodium structure **2**, but for brevity the data for only one of these molecules are highlighted in Table 2. The near equivalence of corresponding O−Li bond lengths across the series is a salient feature. Mean values (and ranges) for **1**−**4** are 1.883 (1.815−1.919), 1.875 (1.833−1.912), 1.886 (1.814−1.933), and 1.893 (1.823−1.934 Å), respectively. Comparison with homonuclear $[(t\text{-BuOLi})_6]$[22] reveals similar O−Li bond lengths (mean, 1.916 Å) within similar trigonal pyramidal LiO_3 localized geometries. Thus the two "O_4Li_2" substructures of **1**−**4** are best regarded as fragments of the $[(t\text{-BuOLi})_6]$ hexamer, and as such their constituent Li^+ centers are "blind" to the fact that their accommodation is heterometallic in composition. It is the retention of these strongly intramolecularly bonded fragments of the all-lithium alkoxide that presumably dictates the breastplate architecture. In this reasoning the plane of four heavier alkali metals provides a positively charged surface onto which the negatively charged $(O_4Li_2)^{2-}$ substructures can dock (Figure 6) through electrostatic forces. This molecular arrangement is therefore best described as a discrete triple ion sandwich. The nature of the interaction with the M_4 plane is the same across the series: there are two

(22) Jetter, P.; Kennedy, A. R.; Mulvey, R. E. Unpublished results.

Table 2. Selected Bond Lengths (Å) and Angles (deg) for Compound **2** (one molecule only)

Bond Lengths			
Na(1)−O(3)	2.3230(17)	Na(1)−O(5)	2.3306(16)
Na(1)−O(1)	2.4955(18)	Na(1)−O(7)	2.5496(18)
Na(2)−O(3)	2.2561(19)	Na(2)−O(6)	2.2676(19)
Na(2)−O(7)	2.5987(19)	Na(2)−O(2)	2.6208(19)
Na(3)−O(4)	2.2774(18)	Na(3)−O(5)	2.2786(17)
Na(3)−O(1)	2.5762(18)	Na(3)−O(8)	2.5978(18)
Na(4)−O(6)	2.3262(18)	Na(4)−O(4)	2.3429(17)
Na(4)−O(8)	2.4553(17)	Na(4)−O(2)	2.5329(18)
Li(1)−O(3)	1.842(4)	Li(1)−O(2)	1.879(4)
Li(1)−O(1)	1.912(4)	Li(2)−O(4)	1.834(4)
Li(2)−O(2)	1.895(4)	Li(2)−O(1)	1.898(4)
Li(3)−O(6)	1.833(4)	Li(3)−O(7)	1.888(4)
Li(3)−O(8)	1.905(4)	Li(4)−O(5)	1.833(4)
Li(4)−O(8)	1.890(4)	Li(4)−O(7)	1.895(4)

Angles			
O(3)−Na(1)−O(5)	160.85(7)	O(3)−Na(1)−O(1)	82.11(6)
O(5)−Na(1)−O(1)	90.02(6)	O(3)−Na(1)−O(7)	88.04(6)
O(5)−Na(1)−O(7)	81.03(6)	O(1)−Na(1)−O(7)	120.87(6)
O(3)−Na(2)−O(6)	161.03(7)	O(3)−Na(2)−O(7)	88.29(6)
O(6)−Na(2)−O(7)	82.03(6)	O(3)−Na(2)−O(2)	81.63(6)
O(6)−Na(2)−O(2)	88.41(6)	O(7)−Na(2)−O(2)	117.53(6)
O(4)−Na(3)−O(5)	161.13(7)	O(4)−Na(3)−O(1)	81.52(6)
O(5)−Na(3)−O(1)	89.20(6)	O(4)−Na(3)−O(8)	87.82(6)
O(5)−Na(3)−O(8)	81.42(6)	O(1)−Na(3)−O(8)	115.68(5)
O(6)−Na(4)−O(4)	161.63(7)	O(6)−Na(4)−O(8)	81.81(6)
O(4)−Na(4)−O(8)	89.84(6)	O(6)−Na(4)−O(2)	89.29(6)
O(4)−Na(4)−O(2)	80.97(6)	O(8)−Na(4)−O(2)	120.90(6)
O(3)−Li(1)−O(2)	118.6(2)	O(3)−Li(1)−O(1)	115.0(2)
O(2)−LI(1)−O(1)	97.50(18)	O(4)−Li(2)−O(2)	116.4(2)
O(4)−Li(2)−O(1)	116.7(2)	O(2)−Li(2)−O(1)	97.43(19)
O(6)−Li(3)−O(7)	118.8(2)	O(6)−Li(3)−O(8)	113.8(2)
O(7)−Li(3)−O(8)	97.58(19)	O(5)−Li(4)−O(8)	117.9(2)
O(5)−Li(4)−O(7)	116.7(2)	O(8)−Li(4)−O(7)	97.87(19)
Li(2)−O(1)−Li(1)	79.73(18)	Li(2)−O(1)−Na(1)	126.57(14)
Li(1)−O(1)−Na(1)	77.56(12)	Li(2)−O(1)−Na(3)	75.65(13)
Li(1)−O(1)−Na(3)	125.70(14)	Na(1)−O(1)−Na(3)	79.70(5)
Li(1)−O(2)−Li(2)	80.67(17)	Li(1)−O(2)−Na(4)	124.52(13)
Li(2)−O(2)−Na(4)	77.19(13)	Li(1)−O(2)−Na(2)	74.06(13)
Li(2)−O(2)−Na(2)	125.21(14)	Na(4)−O(2)−Na(2)	78.64(5)
Li(1)−O(3)−Na(2)	84.55(14)	Li(1)−O(3)−Na(1)	83.55(13)
Na(2)−O(3)−Na(1)	91.44(6)	Li(2)−O(4)−Na(3)	84.95(14)
Li(2)−O(4)−Na(4)	83.48(14)	Na(3)−O(4)−Na(4)	89.97(6)
Li(4)−O(5)−Na(3)	84.56(14)	Li(4)−O(5)−Na(1)	83.39(13)
Na(3)−O(5)−Na(1)	89.69(6)	Li(3)−O(6)−Na(2)	83.94(15)
Li(3)−O(6)−Na(4)	83.75(14)	Na(2)−O(6)−Na(4)	90.63(6)
Li(3)−O(7)−Li(4)	79.98(18)	Li(3)−O(7)−Na(1)	124.59(14)
Li(4)−O(7)−Na(1)	76.33(13)	Li(3)−O(7)−Na(2)	74.07(13)
Li(4)−O(7)−Na(2)	123.92(14)	Na(1)−O(7)−Na(2)	79.11(5)
Li(4)−O(8)−Li(3)	79.69(17)	Li(4)−O(8)−Na(4)	126.85(14)
Li(3)−O(8)−Na(4)	78.81(13)	Li(4)−O(8)−Na(3)	74.89(13)
Li(3)−O(8)−Na(3)	126.86(14)	Na(4)−O(8)−Na(3)	80.49(5)

shorter and two longer O−M bonds per M center involving μ_3-O and μ_4-O centers, respectively. For the shorter bonds mean values are 2.300 (for Na in **2**), 2.643 (for K in **1**), 2.781 (for Rb in **3**), and 2.950 Å (for Cs in **4**). For the longer bonds mean values are 2.553, 2.875, 3.032, and 3.232 Å, respectively. This sequence of increasing O−M bond lengths is accompanied by a similar sequential expansion of the rectangular M_4 planes: mean M···M edge lengths are 3.265, 3.847, 4.059, and 4.279 Å for M = Na, K, Rb, and Cs, respectively. Hence the connectivity within the breastplate structure is independent of the identity and size of the heavier alkali metal partnering lithium. Note also that to construct this architecture, the three largest alkali metals (M = K, Rb, Cs) must depart from the tetrahedral M_4 arrangements of their homonuclear parent structures $[(t\text{-BuOM})_4]$.[5,6] Similarly, the trigonal antiprismatic Na_6 arrangement in $[(t\text{-BuONa})_6]$ must undergo a major reorganization on fragmenting to the planar Na_4 setup encountered in **2**. These dramatic geometrical changes reflect the less "hard" (in the hard acid/soft acid sense), easily polarizable nature of the heavier alkali metals. In contrast, lithium is considerably

Table 3. Selected Bond Lengths (Å) and Angles (deg) for Compound **3**[a]

Bond Lengths			
Rb(1)−O(2)	2.780(3)	Rb(1)−O(5)	2.787(3)
Rb(1)−O(1)	3.030(3)	Rb(1)−O(6)	3.113(3)
Rb(2)−O(4)	2.773(3)	Rb(2)−O(5)	2.784(3)
Rb(2)−O(6)	2.988(3)	Rb(2)−O(3)	3.000(3)
Li(1)−O(2)	1.814(11)	Li(1)−O(6)	1.929(7)
Li(2)−O(4)	1.816(11)	Li(2)−O(6)	1.923(7)
Li(3)−O(5)	1.817(8)	Li(3)−O(1)	1.900(8)
Li(3)−O(3)	1.932(8)		

Angles			
O(2)−Rb(1)−O(5)	144.44(9)	O(2)−Rb(1)−O(1)	91.78(8)
O(5)−Rb(1)−O(1)	68.96(8)	O(2)−Rb(1)−O(6)	67.72(10)
O(5)−Rb(1)−O(6)	88.25(8)	O(1)−Rb(1)−O(6)	105.42(8)
O(4)−Rb(2)−O(5)	146.72(9)	O(4)−Rb(2)−O(6)	69.55(9)
O(5)−Rb(2)−O(6)	90.86(8)	O(4)−Rb(2)−O(3)	90.07(8)
O(5)−Rb(2)−O(3)	68.96(8)	O(6)−Rb(2)−O(3)	105.62(8)
O(2)−Li(1)−O(6)	123.4(3)	O(6)−Li(1)−O(6A)	100.2(5)
O(4)−Li(2)−O(6)	123.2(3)	O(6)−Li(2)−O(6A)	100.6(5)
O(5)−Li(3)−O(1)	125.1(4)	O(5)−Li(3)−O(3)	122.0(4)
O(1)−Li(3)−O(3)	99.2(4)	Li(3)−O(1)−Li(3A)	80.4(5)
Li(3)−O(1)−Rb(1)	77.3(2)	Li(3)−O(1)−Rb(1A)	129.5(3)
Rb(1)−O(1)−Rb(1A)	83.13(9)	Li(1)−O(2)−Rb(1)	88.2(2)
Rb(1A)−O(2)−Rb(1)	92.61(11)	Li(3A)−O(3)−Li(3)	78.8(5)
Li(3)−O(3)−Rb(2)	79.0(2)	Li(3)−O(3)−Rb(2A)	131.6(2)
Rb(2)−O(3)−Rb(2A)	84.65(10)	Li(2)−O(4)−Rb(2)	85.6(2)
Rb(2A)−O(4)−Rb(2)	93.54(11)	Li(3)−O(5)−Rb(2)	87.0(2)
Li(3)−O(5)−Rb(1)	85.4(2)	Rb(2)−O(5)−Rb(1)	94.71(8)
Li(2)−O(6)−Li(1)	78.5(3)	Li(2)−O(6)−Rb(2)	77.8(3)
Li(1)−O(6)−Rb(2)	129.3(3)	Li(2)−O(6)−Rb(1)	128.9(3)
Li(1)−O(6)−Rb(1)	77.0(3)	Rb(2)−O(6)−Rb(1)	84.36(7)

[a] Symmetry transformations used to generate equivalent atoms. A: $x, -y + {}^1/_2, z$.

Table 4. Selected Bond Lengths (Å) and Angles (deg) for Compound **4**[a]

Bond Lengths			
Cs(1)−O(2)	2.9490(17)	Cs(1)−O(5)	2.9529(17)
Cs(1)−O(1)	3.2389(18)	Cs(1)−O(6)	3.3070(18)
Cs(2)−O(4)	2.9437(17)	Cs(2)−O(5)	2.9554(17)
Cs(2)−O(3)	3.1870(18)	Cs(2)−O(6)	3.1970(17)
Li(1)−O(2)	1.823(6)	Li(1)−O(6)	1.927(4)
Li(2)−O(4)	1.830(6)	Li(2)−O(6)	1.934(4)
Li(3)−O(5)	1.823(4)	Li(3)−O(1)	1.919(4)
Li(3)−O(3)	1.933(4)		

Angles			
O(2)−Cs(1)−O(5)	141.58(5)	O(2)−Cs(1)−O(1)	92.27(5)
O(5)−Cs(1)−O(1)	65.16(5)	O(2)−Cs(1)−O(6)	64.05(5)
O(5)−Cs(1)−O(6)	90.77(4)	O(1)−Cs(1)−O(6)	104.54(5)
O(4)−Cs(2)−O(5)	144.48(5)	O(4)−Cs(2)−O(3)	92.26(5)
O(5)−Cs(2)−O(3)	65.04(5)	O(4)−Cs(2)−O(6)	65.56(5)
O(5)−Cs(2)−O(6)	92.92(5)	O(3)−Cs(2)−O(6)	104.68(5)
O(2)−Li(1)−O(6)	125.26(18)	O(6A)−Li(1)−O(6)	100.4(3)
O(4)−Li(2)−O(6)	124.48(19)	O(6)−Li(2)−O(6A)	99.9(3)
O(5)−Li(3)−O(1)	126.6(2)	O(5)−Li(3)−O(3)	123.4(2)
O(1)−Li(3)−O(3)	99.31(18)	Li(3A)−O(1)−Li(3)	80.2(2)
Li(3)−O(1)−Cs(1A)	128.87(15)	Li(3)−O(1)−Cs(1)	77.21(13)
Cs(1A)−O(1)−Cs(1)	82.46(6)	Li(1)−O(2)−Cs(1)	88.78(14)
Cs(1)−O(2)−Cs(1A)	92.75(7)	Li(3)−O(3)−Li(3A)	79.5(2)
Li(3)−O(3)−Cs(2A)	131.79(15)	Li(3)−O(3)−Cs(2)	79.54(13)
Cs(2A)−O(3)−Cs(2)	83.09(6)	Li(2)−O(4)−Cs(2)	87.12(15)
Cs(2)−O(4)−Cs(2A)	91.78(7)	Li(3)−O(5)−Cs(1)	86.69(14)
Li(3)−O(5)−Cs(2)	87.86(14)	Cs(1)−O(5)−Cs(2)	93.11(5)
Li(1)−O(6)−Li(2)	79.16(19)	Li(1)−O(6)−Cs(2)	128.05(18)
Li(2)−O(6)−Cs(2)	78.39(17)	Li(1)−O(6)−Cs(1)	77.04(17)
Li(2)−O(6)−Cs(1)	129.66(18)	Cs(2)−O(6)−Cs(1)	82.51(4)

[a] Symmetry transformations used to generate equivalent atoms. A: $x, -y + {}^1/_2, z$.

Table 5. Crystallographic Data for Compounds **1**−**4**

	1	**2**	**3**	**4**
formula	$C_{32}H_{72}K_4Li_4O_8$	$C_{32}H_{72}Li_4Na_4O_8$	$C_{32}H_{72}Li_4O_8Rb_4$	$C_{32}H_{72}Cs_4Li_4O_8$
fw	769.1	704.6	954.5	1144.3
cryst syst	monoclinic	monoclinic	monoclinic	monoclinic
space group	$P2_1/m$	$P2_1$	$P2_1/m$	$P2_1/m$
crystal color	colorless	colorless	colorless	colorless
a, Å	11.5194(6)	18.998(3)	11.705(3)	12.106(3)
b, Å	17.1506(10)	12.010(3)	17.070(5)	17.080(4)
c, Å	13.0058(7)	20.402(3)	12.957(5)	12.9130(17)
β, deg	110.166(2)	102.899(9)	110.347(19)	109.541(13)
Z	2	4	2	2
T, K	160	160	160	160
$R(F)$ ($F^2 \geq 2\sigma(F^2)$)[a]	0.0324	0.0376	0.0437	0.0230
$wR(F^2)$ (all data)[b]	0.0880	0.0871	0.1088	0.0625
goodness of fit[c]	1.035	0.976	0.904	1.072

[a] $R(F) = \sum||F_o| - |F_c||/\sum|F_o|$. [b] $wR(F^2) = [\sum[w(F_o^2 - F_c^2)^2]/\sum[w(F_o^2)^2]]^{1/2}$. [c] Goodness of fit $= [\sum[w(F_o^2 - F_c^2)^2]/(N-P)]^{1/2}$ for N data and P parameters.

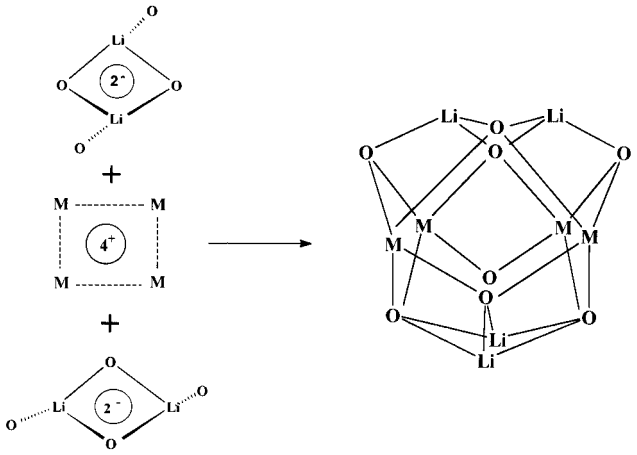

Figure 6. Schematic representation of the construction of the breastplate from its component ions.

"harder" and therefore less coordinatively flexible. Thus it is significant that there is no corresponding lithium−lithium *tert*-butoxide breastplate constructed around a Li_4 plane. Theoretical calculations (vide infra) confirm that the hexameric structure of [(*t*-BuOLi)$_6$] observed experimentally is preferred on thermodynamic grounds. Turning to bond angles within **1**−**4**, a regular trend is found in the pyramidalization of the Li centers. As the interaction of the $[(RO)_4Li_2]^{2-}$ dianions with the $(M_4)^{4+}$ planes gets successively longer and weaker, there is a progressive relaxing of this pyramidalization toward planarity (mean of summed bond angles at Li: 331.1, 343.6, 346.7, and 349.7° for M = Na, K, Rb, and Cs, respectively). For optimum bonding a three-coordinate Li center would be trigonal planar; hence from this perspective it can be reasoned that enlarging the size of the "belly" (M_4 section) of the breastplate structure helps to alleviate steric strain (i.e., the Cs system, **4**, represents the least strained of the series). It is also apparent that the bond angles subtended at Li are arranged in two groups: within the $(OLi)_2$ ring they are fairly constant, typically about 100°; but outside this ring a substantial widening and greater range (113.8−126.6°) are observed. Bond angles at each of the M centers come in three distinct categories depending on the combination of bridging indices of the attached O centers: μ_3O−M-μ_3O; μ_4O−M-μ_4O; and μ_3O−M-μ_4O. The first category display the widest angles, ranging from a mean lower limit of 143.0° when M = Cs to a mean upper limit of 161.2° when M = Na. The second category is intermediate in width, and again the smallest and largest mean values occur at Cs (104.6°) and Na (118.7°), respectively. Constrained within four-membered rings, the third category display the narrowest angles. These can be subdivided into those in $(OM)_2$ rings, which show little variance across the series (typically about 90°), and those in (OMOLi) rings, which follow the same trend as found in the previous two categories (smallest at Cs, largest at Na: mean values, 64.9 and 81.5°, respectively). Thus it is the mismatch in size between small Li^+ and its larger M^+ partner that causes the greatest endocyclic angular distortion at the metal corners. By comparison there is less of a spread in bond angles at the O centers within the four-membered rings. Those at the μ_3-O centers cover a range of 83.39−94.71° across the series. In general, sharper bond angles are observed at the μ_4-O centers, though again the range (74.06−84.65°) is limited across the series.

Theoretical Calculations. We have used ab initio MO calculations [23] to assess the relative energetics of the breastplate architecture against those of its homonuclear component structures. For calculational simplicity the *t*-BuO$^-$ anions of the experimental breastplate were substituted by MeO$^-$ anions in the tetralithium−tetrasodium model [$(MeO)_8Li_4Na_4$], **2A**. The geometry optimizations were carried out initially at the Hartree−Fock level using the 6-31G* basis set[24a] and the status of the minimum energy geometry evaluated by a frequency analysis. The geometry was then refined using the density functional theory (B3LYP) model[25] with the 6-311G(**)[24b] basis set. The energy and structural parameters emanating from the latter calculations are presented herein. This molecule (Figure 7), which was freely refined without the imposition of any geometrical constraints, optimizes to D_{2d} symmetry and simulates exactly the connectivity pattern found in the crystal structure of **2**. There is also a reasonable agreement between the bond lengths in **2A** and **2**, though the calculated ones tend to be marginally foreshortened by comparison. Illustrating this point: the μ_3O−Li and μ_4O−Li bond lengths in **2A** are only 0.015 and 0.003 Å shorter respectively than the mean such bonds in **2**; the μ_3O−Na and μ_4O−Na bond lengths in **2A** are only 0.017 and 0.082 Å shorter respectively than the mean such bonds

(23) Gaussian 94 (Revision A.1), Frisch, M. J.; Trucks, G. W.; Schlegel, H. B.; Gill, P. M. W.; Johnson, B. G.; Robb, M. A.; Cheeseman, J. R.; Keith, T. A.; Peterson, G. A.; Montgomery, J. A.; Raghavachari, K.; Al-Laham, M. A.; Zakrzewski, V. G.; Ortiz, J. V.; Foresman, J. B.; Cioslowski, J.; Stefanov, B. B.; Nanayakkara, A.; Challacombe, M.; Peng, C. Y.; Ayala, P. Y.; Chen, W.; Wong, M. W.; Andres, J. L.; Replogle, E. S.; Gomperts, R.; Martin, R. L.; Fox, D. J.; Binkley, J. S.; Defrees, D. J.; Baker, J.; Stewart, J. P.; Head-Gordon, M.; Gonzalez, C.; Pople, J. A.; Gaussian, Inc.: Pittsburgh, PA, 1995.

(24) (a) Hehre, W. J.; Ditchfield, R.; Pople, J. A. *J. Chem. Phys.* **1972**, *56*, 2257. Hariharan, P. C.; Pople, J. A. *Theor. Chim. Acta* **1973**, *28*, 213. Dill, J. D.; Pople, J. A. *J. Chem. Phys.* **1975**, *62*, 2921. (b) McLean, A. D.; Chandler, G. S. *J. Chem. Phys.* **1980**, *72*, 5639.

(25) Becke, D. A. *J. Chem. Phys.* **1993**, *98*, 5648.

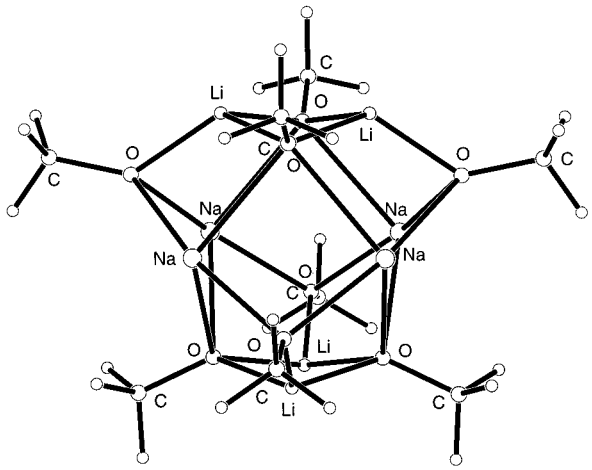

Figure 7. Ab initio MO geometry-optimized structure of the model breastplate $[(MeO)_8Li_4Na_4]$, **2A**.

Table 6. Selected Bond Lengths (Å) and Angles (deg) for Model **2A**

	Bond Lengths		
Li−μ_3O	1.820	Na−μ_3O	2.282
Li−μ_4O	1.892	Na−μ_4O	2.471
		Na···Na	3.149
	Angles		
μ_3O−Li-μ_4O	116.0	Na−μ_3O−Li	83.1
μ_4O−Li-μ_4O	95.1	Na-μ_3O−Na	87.1
sum around Li	327.1	Na−μ_4O−Na	79.2

in **2**; and the Na···Na edge length in **2A** is only 0.116 Å shorter than the mean such length in **2**. Table 6 lists relevant bond lengths and bond angles in **2A**. Note that the staggered arrangement of the $(O_4Li_2)^{2-}$ rings with respect to each other is more critical to the stability of **2A** than the planar Na_4 arrangement, twisting these rings into an eclipsed conformation reduces the stability significantly (by 20.7 kcal mol^{-1}), whereas rotating the Na atoms by 45° causes them to assume a tetrahedral geometry with a loss of stability of only 8.4 kcal mol^{-1}.

The model homonuclear structures $[(MeOLi)_6]$ and $[(MeONa)_6]$ were also optimized using the same basis set. These hexamers adopt similar D_{3d} trigonal antiprismatic arrangements [made up of two stacked $(OLi)_3$ rings]. From their total energies (−736.748123 and −1665.241354 au, respectively) and that of **2A** (−1601.358491 au) an approximate energy of formation (ΔE_f in kcal mol^{-1}) can be calculated, based on the hypothetical reaction expressed in eq 2. The value obtained (−20.2 kcal mol^{-1}) reveals that the reaction is highly exothermic, and establishes that the driving force for the formation of the mixed-metal breastplate from its homonuclear components is thermodynamic. The increase in the number of O−Na bonds (per Na center) from three in $[(MeONa)_6]$ to four in **2A** must contribute significantly to this exothermicity.

$$^2/_3[(MeOLi)_6] + {}^2/_3[(MeONa)_6] \rightarrow [(MeO)_8Li_4Na_4]$$

$$\Delta E_f = -20.2 \text{ kcal mol}^{-1} \quad (2)$$

As alluded to earlier, it is interesting to ponder on why no analogous lithium−lithium *tert*-butoxide breastplate has been observed experimentally. This prompted the construction of a theoretical model $[(MeO)_8Li_4Li_4]$, the total energy of which was calculated to be −982.321483 au. As revealed in eq 3, this alternative structure is less stable (by 4.4 kcal mol^{-1}) than the known hexameric arrangement. A major contributory factor to this instability is the relative weakness of the O−Li bonds emanating from the Li_4 plane in the midriff of the breastplate. Two are exceedingly long at 2.214 Å, while the remaining two (at 1.979 Å) are still longer than all those (2 × 1.886 Å, 1.925 Å) in $[(MeOLi)_6]$. Therefore, although the midriff Li centers gain in terms of coordination number (4 versus 3 in $[(MeOLi)_6]$), the implication is that the $(Li_4)^{4+}$ plane is too small to support the two $(O_4Li_2)^{2-}$ subunits effectively. While the O−Li bond lengths within these subunits are considerably stronger (lengths: 2 × 1.862 Å; 1.810 Å), their μ_3-Li centers must sustain a greater pyramidal distortion [sum of bond angles, 310.7°; cf. 327.1° in $(MeOLi)_6$] to effect the attachment to the Li_4 plane. This greater pyramidalization follows the trend described above for the experimental breastplates (i.e., as the M_4 plane gets larger, there is a gradual shift toward planarity). Concomitant with the greater pyramidalization, the O centers crowd together more in $[(MeO)_8Li_4Li_4]$ than they do in $[(MeOLi)_6]$ (shortest O···O separations: 2.714/2.982 Å and 2.908/3.392 Å, respectively).

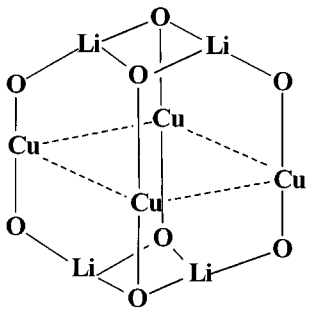

Figure 8. Schematic representation of the molecular structure of $[(t\text{-BuO})_8Li_4Cu_4]$, **5**.

$$[(MeOLi)_6] \rightarrow {}^3/_4[(MeO)_8Li_4Li_4]$$

$$\Delta E_f = +4.4 \text{ kcal mol}^{-1} \quad (3)$$

This set of calculations has underlined the stability of the breastplate architecture and raises the question, "is this 16-vertex cage arrangement of significance in any other areas of structural chemistry?" The following section addresses this question.

The Extended Breastplate Family. Searching for possible relatives of this structural family, one is immediately drawn to the mixed lithium−copper alkoxide $[(t\text{-BuO})_8Li_4Cu_4]$, **5**.[26] It has an identical stoichiometry and composition to **1**−**4** with Cu(I) centers replacing the heavier alkali metal components. There are also clear similarities between the structure of **5** (Figure 8) and those of **1**−**4**. Most pertinently, the four Cu centers occupy a perfect plane, to which are attached two $(O_4Li_2)^{2-}$ subunits. But a significant distinction is also evident: each Cu center binds to only one O center from each of these $(O_4Li_2)^{2-}$ subunits. The result is near-linear (175.5−175.6°) O−Cu−O bridges. Thus the cage connectivity is different from that in **1**−**4**, being composed of $2(OLi)_2$ rings and 4 eight-membered $(LiOCuO)_2$ rings instead of 14 four-membered rings. Furthermore, the $(OLi)_2$ rings in **5** must align themselves in an approximately eclipsed fashion to effect the linear O−Cu−O bridging, whereas in **1**−**4** a staggered arrangement is observed. It should be pointed out that both copper and lithium strongly influence this alternative architecture of **5**: the Cu(I) centers attain their preferred two-coordinate linear geometry; while the Li centers maintain the three-coordinate pyramidal geometry

(26) Purdy, A. P.; George, C. F. *Polyhedron* **1995**, *14*, 761.

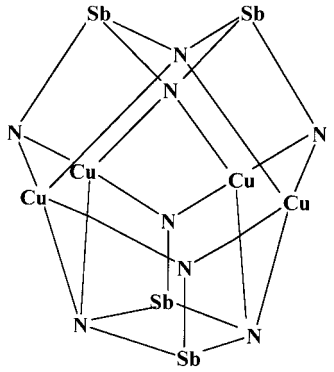

Figure 9. Schematic representation of the molecular structure of $[(CyN)_8Sb_4Cu_4]$.

adopted in **1**−**4**. The crucial difference with **5** is the way in which the Cu centers utilize the $(O_4Li_2)^{2-}$ subunits as multidentate ligands: in **5** they act as four monodentate sources, whereas in **1**−**4** they act as four bidentate sources (to M centers). Thus it is the coordinative flexibility of the O donor atoms (μ_3/μ_4-bonded in **1**−**4**; μ_2/μ_3-bonded in **5**) within these subunits that lays the foundation for the structure of **5**. The same comments apply to the structure of the mixed sodium−copper alkoxide $[(Et_3CO)_8Na_4Cu_4]$[26] which is practically identical to that of **5**.

There are, however, even closer analogues to the breastplate structure. These turn up unexpectedly in a set of heterometallic compounds which contain neither alkoxide ligands nor, in most cases, alkali metal cations. Reported by the Wright group, they have a general formula of $[(CyN)_8M^1{}_4M^2{}_4]$, where M^1 = Sb or As and M^2 = Ag, Cu, or Na.[27] Representative of this type, the structure of the mixed tetraantimony−tetracopper imide[27a] is shown in Figure 9. Mimicking the heavier alkali metal cations of **1**−**4**, its four Cu centers generate a perfect plane. Straddling this plane are two $(Sb_2N_4)^{2-}$ dianions disposed orthogonal to each other, which simulate the role of the $(Li_2O_4)^{2-}$ dianions in **1**−**4**. The pendant N arms of each $(Sb_2N_4)^{2-}$ dianion form short Cu−(μN)−Cu interactions at opposite edges of the Cu_4 plane, which can be compared to the μ_3O−M interactions in **1**−**4**. Similarly, longer range Cu···(μN)···Cu interactions involving the μN centers of the $(SbN)_2$ puckered rings can be compared to the μ_4O−M interactions in **1**−**4**. Therefore there is an exact match in connectivity between the imide and the alkoxide cage systems. However, the margin of difference in length between the short and long N−Cu bonds (about 1 Å) far exceeds the corresponding values for the O−M bonds in **1**−**4**. This distinction can be attributed to the greater pyramidalization at the Group 15 metal center caused by the strongly repulsing, exo-oriented lone pair. Also located at the periphery of the cage, one "R" group (cyclohexyl) per N center completes the structure. This is comparable to the one *tert*-butyl group per O center in the butoxide breastplate.

Surveying the compositions of the imide series, it is clear that several factors contribute toward this isostructural relationship with **1**−**4**: (i) imide (RN^{2-}) ligands are isoelectronic with alkoxide (RO^-) ligands; (ii) by containing an equal number of 'R' substituents steric influences are minimized; (iii) $[As_2(NR)_4]^{2-}$ and $[Sb_2(NR)_4]^{2-}$ are isovalent (contributing 24 electrons to the cage discounting the tangential lone pairs on As and Sb and the two electrons filling the N−R bonds) with $[Li_2(OR)_4]^{2-}$; (iv) these complex anions carry the same net charge (2−); and (v) the tetrametal midriff planes each carry a formal charge of 4+. It is noteworthy that the mixed tetraantimony−tetralithium imide $[(CyN)_8Sb_4Li_4]$[28] does not adopt a breastplate architecture, as its Li_4 substructure is tetrahedral, not planar. This is consistent with the results of the MO calculations outlined above which predict that an Li_4 plane is too small an electrophilic surface to support large tetradentate nucleophiles. In an excellent review[29] it is suggested that the architectures of these imides and related heterometallic alkali metal/p-block metal compounds are governed mainly by the greater covalency of the p-block metal−ligand interactions. While all-alkali metal complexes must be inherently more ionic overall, this interpretation is not inconsistent with the breastplate structures described here. To elaborate, O−Li bonds have a higher degree of covalency than their heavier alkali metal counterparts, hence the reason why in **1**−**4** lithium commands the structure-directing role of the p-block metals.

Concluding Remarks. To the best of our knowledge, there is no precedent for an isostructural homologous series in alkali metal organoelement chemistry. It follows that **1**−**4** also constitutes the first isostructural homologous series of alkali metal-based heterometallic compounds. Looking for reasons why this unique isostructural relationship should hold here, one can point to the retention of the strongly intramolecularly bonded $(O_4Li_2)^{2-}$ dianions as a major factor. The ability of these tetradentate dianions to function as ligands and to adapt their stereochemistry to suit the significant size differences of the heavier alkali metal $(M^+)_4$ planes are also contributory factors. This stereochemical flexibility appears to be largely controlled by the versatility of lithium to tolerate a range of coordinative geometries through trigonal pyramidal to trigonal planar. For their part, the heavier alkali metals, being of diminished hardness relative to lithium, readily submit to an unaccustomed coplanar environment because it best satisfies the multi-coordinative needs of the dianionic ligands. There is clearly a remarkable resemblance between the structures of **1**−**4** and those of the series of heterometallic p-block metal-based imide structures. Given that the origin of this structural similarity probably stems from their common dianion−tetramonocation−dianion, contacted triple ion sandwich arrangement, it is reasonable to assume that other heterometallic compounds having this arrangement, but yet to come to light, will adopt the breastplate or pseudo-breastplate architectures. It must also be stressed that, while the breastplate is made up of three ionic sections, individual bonds within and between these sections can have a significant degree of covalent character as exemplified by the p-block metal-containing imides.

Experimental Section

Reactions were carried out in Schlenk tubes under a protective, dry argon atmosphere. Pure shield argon was purchased from BOC Gases. Crystalline products were transferred to an argon-filled glovebox for storage and subsequent characterization. The metal alkoxides *t*-BuOLi, *t*-BuONa, and *t*-BuOK were obtained commercially from Aldrich; *t*-BuORb and *t*-BuOCs were prepared according to literature methods.

(27) (a) Barr, D.; Edwards, A. J.; Pullen, S.; Paver, M. A.; Raithby, P. R.; Rennie, M.-A.; Russell, C. A.; Wright, D. S. *Angew. Chem.* **1994**, *106*, 1960; *Angew. Chem., Int. Ed. Engl.* **1994**, *33*, 1875. (b) Beswick, M. A.; Cromhout, N. L.; Harmer, C. N.; Paver, M. A.; Raithby, P. R.; Rennie, M.-A.; Steiner, A.; Wright, D. S. *Inorg. Chem.* **1997**, *36*, 1740. (c) Bashall, A.; Beswick, M. A.; Harmer, C. N.; Hopkins, A. D.; McPartlin, M.; Paver, M. A.; Raithby, P. R.; Wright, D. S.; *J. Chem. Soc. Dalton Trans.* **1998**, 1389. (d) Bashall, A.; Beswick, M. A.; Harron, E. A.; Hopkins, A. D.; Kidd, S. J.; McPartlin, M.; Raithby, P. R.; Steiner, A.; Wright, D. S. *Chem. Commun.* **1999**, 1145.

(28) Alton, R. A.; Barr, D.; Edwards, A. J.; Paver, M. A.; Raithby, P. R.; Rennie, M. A.; Russell, C. A.; Wright, D. S. *J. Chem. Soc., Chem. Commun.* **1994**, 1481.

(29) Beswick, M. A.; Mosquera, M. E. G.; Wright, D. S. *J. Chem. Soc., Dalton Trans.* **1998**, 2437.

Solvents were distilled over sodium/benzophenone until blue, directly placed over fresh 4A molecular sieves, then degassed by the freeze−pump−thaw procedure. ^{1}H NMR spectral data were recorded on a Bruker AMX 400 spectrometer operating at 400.13 MHz, using C_6D_5-CD_3 solutions at ambient temperature; chemical shifts are quoted relative to external $SiMe_4$.

Preparation of [(*t*-BuO)$_8$Li$_4$K$_4$] (1). The solid homometallic alkoxides *t*-BuOLi (0.32 g, 4 mmol) and *t*-BuOK (0.23 g, 2 mmol) were mixed together in a Schlenk tube and stirred dry for 15 min. Toluene (5 mL) was added to give an almost transparent solution, which was then heated to ca. 70 °C for 20 min. After cooling the resulting yellow solution, TMEDA (0.52 mL, 4 mmol) was added and the mixture was stirred for 1 h. The solution was then surrounded by a hot water bath and pumped to dryness in vacuo to leave a greasy yellow residue. Hexane (5 mL) was added to the residue to give a slightly turbid yellow solution, which was subsequently filtered. Cooling the filtrate to −26 °C for 48 h afforded colorless crystals of **1**. Yield of first batch, 32%. On keeping the filtrate and recooling, an improved yield of 40% was obtained. Mp 242 °C. ^{1}H NMR: δ 1.24 (s, 36H, *t*-BuO), 1.31 (s, 36H, *t*-BuO).

Preparation of [(*t*-BuO)$_8$Li$_4$Na$_4$] (2). The procedure described above for **1** was followed with *t*-BuONa replacing *t*-BuOK. Furthermore the *t*-BuOLi:*t*-BuONa:TMEDA stoichiometry employed was 1:1:1. Heterometallic **2** was obtained as colorless crystals. Yield of first batch, 16%. On keeping the filtrate and recooling, an improved yield of 51% was obtained. Mp 270−272 °C. ^{1}H NMR: δ 1.33 (s, 72H, *t*-BuO).

Preparation of [(*t*-BuO)$_8$Li$_4$Rb$_4$] (3). The procedure described above for **1** was followed with *t*-BuORb replacing *t*-BuOK. Furthermore the *t*-BuOLi:*t*-BuORb:TMEDA stoichiometry employed was 2:1:2. Heterometallic **3** was obtained as colorless crystals. No yield nor melting point could be obtained as this product (and subsequent repeat products) were found to be contaminated with a hydroxide-containing side product (OH resonance in ^{1}H NMR appeared at δ −2.24). ^{1}H NMR: δ 1.24 (s, 36H, *t*-BuO), 1.31 (s, 36H, *t*BuO).

Preparation of [(*t*-BuO)$_8$Li$_4$Cs$_4$] (4). The procedure described above for **1** was followed with *t*-BuOCs replacing *t*-BuOK. Furthermore the *t*-BuOLi:*t*-BuOCs:TMEDA stoichiometry employed was 2:1:2. Heterometallic **4** was obtained as colorless crystals. Yield of first batch, 21%. Mp 142 °C. ^{1}H NMR: δ 1.30 (s, 72H, *t*-BuO).

X-ray Crystallography. Crystal samples were mounted using oil-drop techniques. Crystal data and refinement parameters are given in Table 5, and selected geometric parameters are given in Tables 1−4.

Crystals were examined on a Bruker AXS SMART CCD diffractometer with graphite-monochromated Mo Kα radiation ($\lambda = 0.71073$ Å).[30] Data (over a hemisphere in each case) were corrected semiempirically for absorption. The structures were solved by direct methods [31] and refined by least squares on all unique F^2 values, with anisotropic non-hydrogen atoms and with constrained isotropic H atoms. There were no significant features in final difference maps.

Acknowledgment. We thank the University of Strathclyde for funding this research project and the UK EPSRC for partial funding of the X-ray diffraction equipment.

Supporting Information Available: Tables of crystal data, structure solution and refinement, atomic coordinates and equivalent isotropic displacement parameters, bond lengths and angles, anisotropic displacement parameters, and hydrogen atom coordinates and isotropic displacement parameters for rem218, rem259, rem250, and rem282 (PDF). Full crystallographic details including atomic coordinates, thermal parameters, bond lengths and angles, and atomic displacement parameters for compounds **1**−**4** (CIF). This material is available free of charge via the Internet at http://pubs.acs.org.

JA002217Z

(30) SMART and SAINT software for CCD diffractometers, Bruker AXS Inc.: Madison, Wisconsin, 1997.

(31) G. M. Sheldrick, SHELXTL manual, version 5, Bruker AXS Inc.: Madison, Wisconsin, 1997.